Polarization of the mouse node cells by asymmetric distribution of Wnt5a/5b and their inhibitor

（*Wnt5a/5b* と *Wnt* のアンタゴニストの非対称性の分布がノードの細胞極性を決めている）

March 2015

（平成 27 年 3 月）

Developmental Genetics Groups (Hamada's Laboratory)

Graduate School of Frontier Biosciences

Osaka University

大阪大学大学院生命機能研究科

指導教官 濱田博司教授

Katsura Minegishi

峰岸 かつら

COCNTENTS

SUMMARY

The leftward fluid flow in the node is responsible for the breaking of left-right symmetry in mouse embryo. The unidirectional fluid flow is generated by rotation of posteriorly tilted cilia in the node. The tilt of cilia is determined by the position of the basal body of node cell. It has been established that the PCP pathway controls the basal body positioning in node cells. However, it is unclear how initial global A-P axis regulates the polarized distribution of core PCP proteins in node cells. Mainly using mouse genetics, we have examined the role of non-canonical Wnt signaling in node cell polarity. The position of the basal body was affected by the lack of Wnt5a/5b genes. It was also surprising that the basal body failed to shift posteriorly in Sfrp1/2/5 mutant. Moreover, mutant embryos and uniform Wnt5a-expressing embryos showed the same basal body positioning defect. Our results suggest that a combination of the posteriorly-expressed *Wnt5a/5b* and anteriorly-expressed *Sfrps* would generate gradient of Wnt5 activity. This activity would be responsible for cell polarity in the node.

INTRODUCTION

It is important to establish the anteroposterior (AP), dorsoventral (DV), and left-right (LR) axes for the vertebrate body plan formation. There are five key steps that contribute to the establishment of left-right (LR) patterning in the mouse (Fig 1 (a)). The first step is the symmetry-breaking event that takes place in the node cavity in early embryogenesis. During this step, in the node cavity, 200-300 motile cilia rotating in clock-wise direction generate an unidirectional (leftward) fluid flow referred to as "nodal flow". This might be explained by the rotational axis of each cilium which is tilted toward the posterior side (Cartwright et al., 2004; Nonaka et al., 1998; Nonaka et al., 2005) (Fig 1 (b), Fig2 a). The position of the basal body gradually shifts toward the

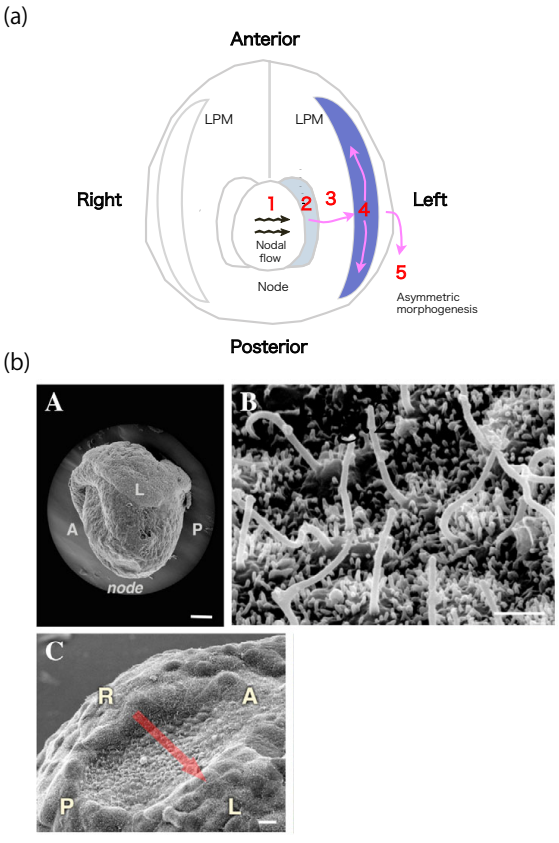

Figure 1. Five steps for Left-Right determination

(a) Schematic diagram of L-R asymmetry breaking at E7.5 of mouse embryo from ventral view. 1: Generation of nodal flow, 2: Sense and conversion of asymmetric signal at the edge of the node, 3: Transmission of asymmetric signal from node to left lateral plate mesoderm (LPM), 4: Extension of Nodal signal at LPM, 5: Asymmetric morphogenesis (reprinted from Yoshiba, S. thesis for doctoral degree 2012). **(b)** (A) Lateral view of a mouse embryo at E7.5 dpc. Scale bar: 100 μ m, (B) Monocilia in the node of a mouse embryo shown at high magnification. Scale bar: 100 μ m, (C) Ventral view of the node cavity and direction of the nodal flow (red arrow). Scale bar: 100 μ m , reprinted from (Shiratori and Hamada, 2006).

posterior side of node cells and reaches the most posterior side around three-somite stage (Fig 2 c). Because of the relatively rounded shape of node cell, basal bodies located at the posterior side would result in posteriorly tilted cilia (Fig2 a, c). (Nonaka et al., 1998; Nonaka et al., 2005)

Originally characterized in Drosophia, the planar cell polarity (PCP) pathway,

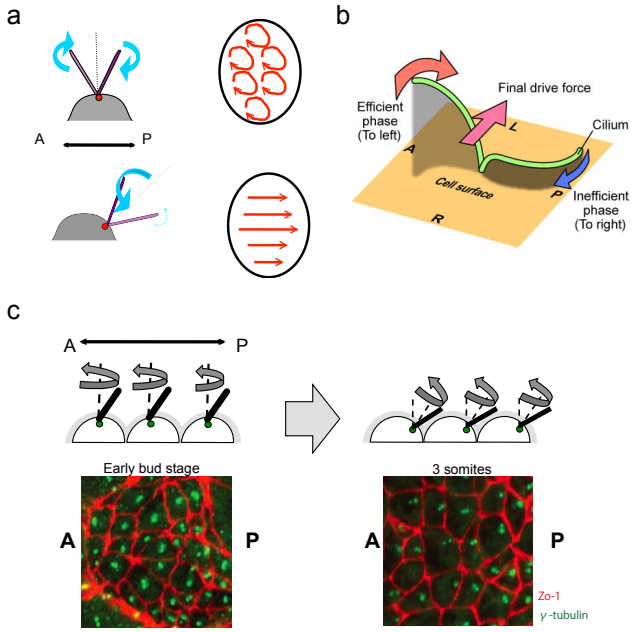

Figure 2. Directional leftward flow is generated by circular clock-wise motion of cilia

(a) and (b) Representation of Nodal flow generation. **(a)** Circular clockwise motion of a cilium can generate directional leftward flow if its axis is not perpendicular to the cell surface but tilted posteriorly. **(b)** Due to its distance from the cell surface, a cilium in the leftward phase (red arrow) drags surrounding water more efficiently than the rightward phase (blue arrow), resulting in a global leftward force (purple arrow), reprinted from (Nonaka et al., 2005). **(c)** Basal body gradually shifts toward the posterior side in the node cell and is found on the most posterior side at tree-somite stage as indicated by the illustration and the immunostaing(γ -tubulin: green; Zo-1: red).

is regulated by the evolutionarily-conserved genes called to as “PCP core proteins”. Some of these proteins, such as Dvl, Vangl1 and Prickle, are asymmetrically distributed in node cells along the anterior-posterior (A-P) axis. Moreover, the positioning of the basal body is impaired in mutant mice lacking each Dvl and Vangl genes ((Antic et al., 2010; Hashimoto et al., 2010; Song et al., 2010). Therefore the posterior positioning of the basal body is determined by the PCP signaling pathway.

Presumably, a pre-existing A-P positional information would be translated by node cells and be used to induce polarized localization of PCP core proteins. However, it

is unclear how initial global A-P axis regulates the polarized distribution of core PCP proteins in node cells (Fig3). Recent studies have shown the involvement of noncanonical Wnt-regulated PCP in various vertebrate developmental processes, such as convergence and extension gastrulation movements (Gao et al., 2011; Heisenberg et al., 2000; Qian et al., 2007). It is possible that Wnt ligand-dependent or -independent mechanisms induce the polarized localization of PCP core proteins in node cells. In this paper, mainly using mouse genetics, we have examined the role of non-canonical Wnt signaling in node cell polartization. Our findings showed that posteriorly-expressed Wnts are required for node cell polarization.

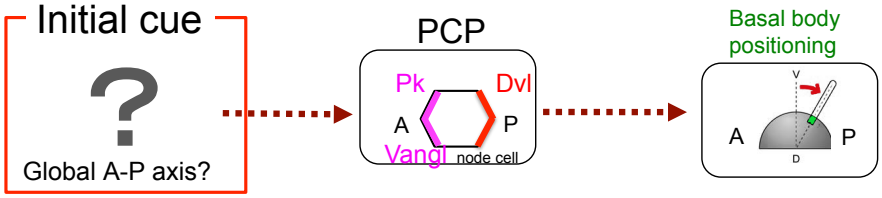

Figure 3. How dose initial A-P axis regulate the polarized distribution of core PCP proteins in node cells?

PCP pathway controls the positioning of the basal body in node cells. But initial cues regulating PCP pathway in

RESULTS

PCP core proteins Prickle1 and Prickle2 are required for correct positioning of the node cilia

Prickle1 and *Prickle2* are expressed in the ventral node (Fig 4 a) and Prickle2 protein shows polarized localization at the anterior side of node cells (Fig 4 b, Fig 5 b) (Antic et al., 2010). However, function of Prickle proteins in the node remains unknown. Prickle1 deletion in the mouse leads to embryonic lethality due to defects of the apicobasal polarity in epiblast followed by gastrulation defects (Tao et al., 2009). To determine whether Prickles are involved in the positioning of node cilia, we generated Prickle1 and Prickle2 mutant mice by deleting the exon 6 (Fig S1). Prickle2 $^{\Delta ex6/\Delta ex6}$ mice had no phenotype. Unlike Prickle1 null mouse that are embryonic lethal, Prickle1$^{\Delta ex6/\Delta ex6}$ mice were born but died within 24 hours after birth, suggesting that the Δex6 allele is hypomorphic. In several *Prickle1*$^{\Delta ex6/\Delta ex6}$ *Prickle2* $^{\Delta ex6/\Delta ex6}$ embryos, Nodal flow displayed multiple vortical flow (Fig4 c). We then examined the average basal body position (ABP)(Hashimoto et al., 2010). The ABP represents the relative position of the basal body in each cell along the A-P axis. The anterior and posterior ends of a cell are represented by –1.0 and +1.0 respectively (Fig S2) (Hashimoto et al., 2010). The ABP was significantly decreased in *Prickle1*$^{\Delta ex6/\Delta ex6}$ *Prickle2* $^{\Delta ex6/\Delta ex6}$ node cells (Fig4 d, e, f), suggesting that the basal body failed to shift posteriorly.

To clarify the relation between Prickle and Vangl, we examined the localization of Vangl1 protein in node cells of Prickle1$^{\Delta ex6/\Delta ex6}$ Prickle2 $^{\Delta ex6/\Delta ex6}$ embryos. As reported previously(Song et al., 2010), Vangl1 is asymmetrically distributed at A-P boundaries in node cells. Observation of Vangl1 localization at a higher resolution

showed that it is indeed localized at the anterior end of node cells (Fig5 a). The asymmetric distribution of Vangl1 at both A-P and left-right boundaries of cells was observed in *Prickle1*$^{\Delta ex6/\Delta ex6}$ *Prickle2* $^{\Delta ex6/\Delta ex6}$ node (Fig6 a,b). Using Vangl1 staining

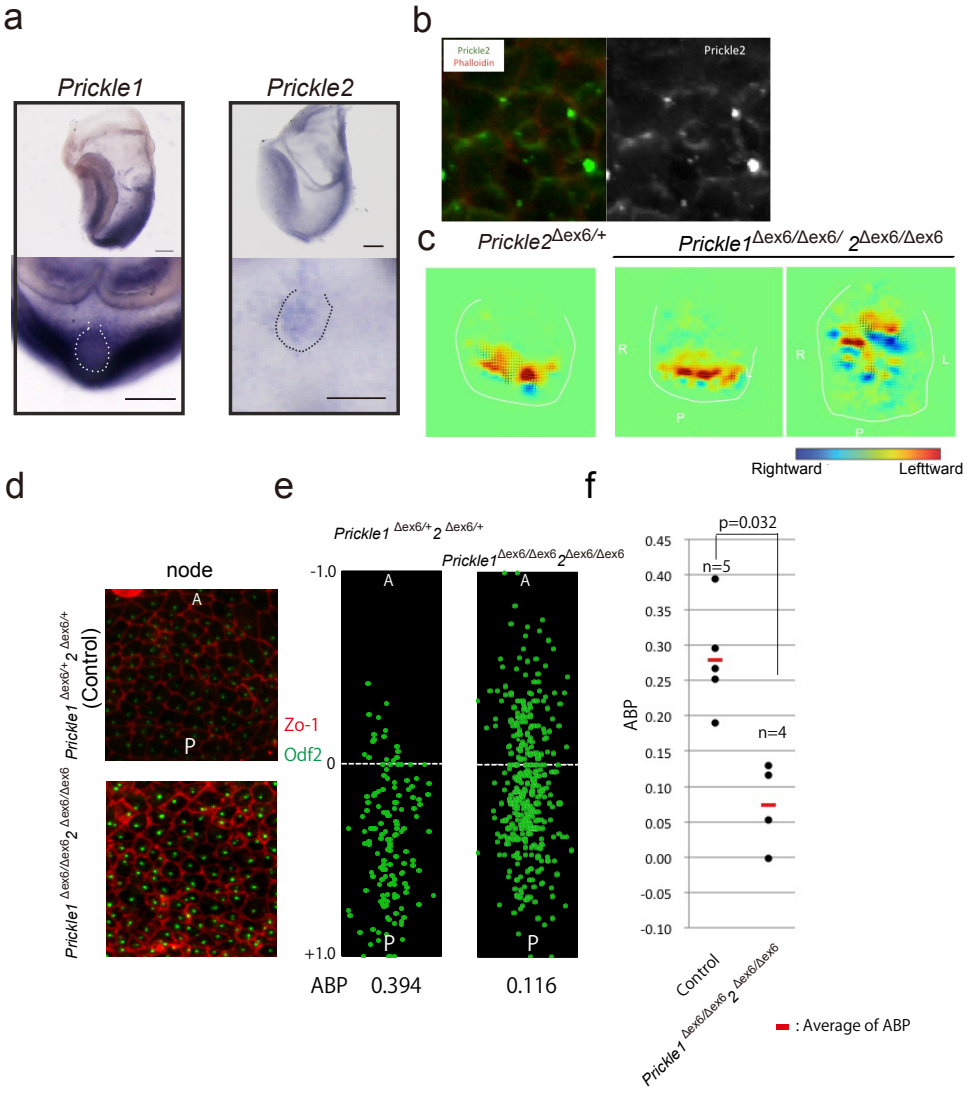

Figure 4. Prickle1 and 2 play a key role in the positioning of node cilia

(a) Whole-mount in situ hybridization analysis of E7.5 WT mouse embryo with *Prickle1* and *2*. The dotted lines indicate the node position. Scale bars: 100 μ m. **(b)** Immunofluorescence staining of Prickle2 (green and gray) and Phalloidin (red) in the node. **(c)** PIV analysis of nodal flow by the movement of fluorescent microbeads. The white line indicates the shape of node. Each arrow denotes the direction and velocity of the flow at the indicated position. Relative colour scale indicates the magnitude of the flow velocity (leftward in yellow/red, and rightward in blue). **(d)** Immunostaining of Zo-1 (red) and Odf2 (green) in the control and *Prickle1*$^{\Delta ex6/\Delta ex6}$ *Prickle2* $^{\Delta ex6/\Delta ex6}$ node at 3-5 So stages. **(e)** A-P relative position of the basal body (green dots) in node of control and *Prickle*$^{-/-}$*2*$^{-/-}$ embryos at 3-5 So stages and corresponding ABP rate. **(f)** The ABP is impaired in *Prickle1*$^{\Delta ex6/\Delta ex6}$ *Prickle2* $^{\Delta ex6/\Delta ex6}$ (n=4) as compared to control node (n=5) at 3~5So stage (two-tail t test, p = 0.032). A, anterior; P posterior; R, right; L, left.

signal, we measured the positive cell borders orientation in reference to the A-P axis. Depending on the values, cell boundaries were labeled as horizontal (angle between $0^{\circ} \sim 45^{\circ}$, $135^{\circ} \sim 225^{\circ}$ and $315^{\circ} \sim 360^{\circ}$) or vertical (angle between $45^{\circ} \sim 135^{\circ}$ and $225^{\circ} \sim 315^{\circ}$) and the proportion between those two populations were estimated by a H/V rate (Fig S3). The H/V rate was significantly reduced in Prickle1$^{\Delta ex6/\Delta ex6}$ Prickle2 $^{\Delta ex6/\Delta ex6}$ embryos (Fig6 a, b). This result indicated that Prickle 1 and 2 play a key role in the positioning of node cilia and is also involved in the localization of Vangl1 in node cells.

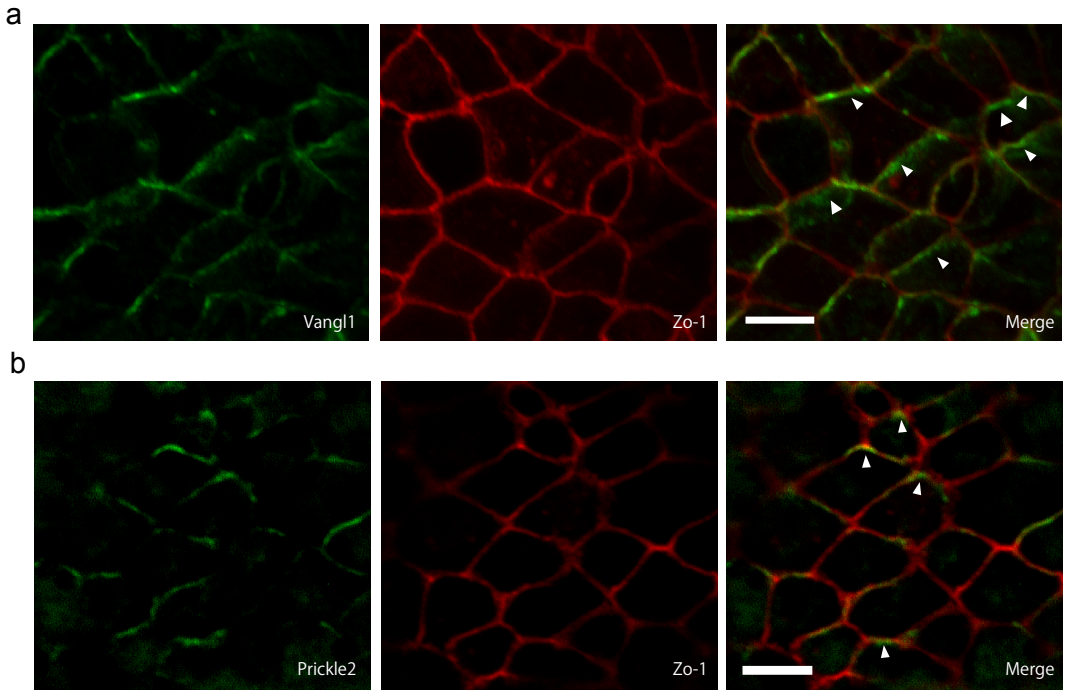

Figure 5. Observation of Vangl1 and Prickle2 localization at a higher resolution
Immunostaining of **(a)** Vabgl1 (green) and Zo-1 (red) and **(b)** Prickle2 (green) and Zo-1 (red) in the node. The images were taken by the Olympus Super Resolution software (FV-OSR) and the high-sensitivity detector (FV12-HSD) with the FV-1000 confocal microscope. Scale bars: 5 μ m.
Arrow heads indicate the anterior distribution of each protein in node cells.

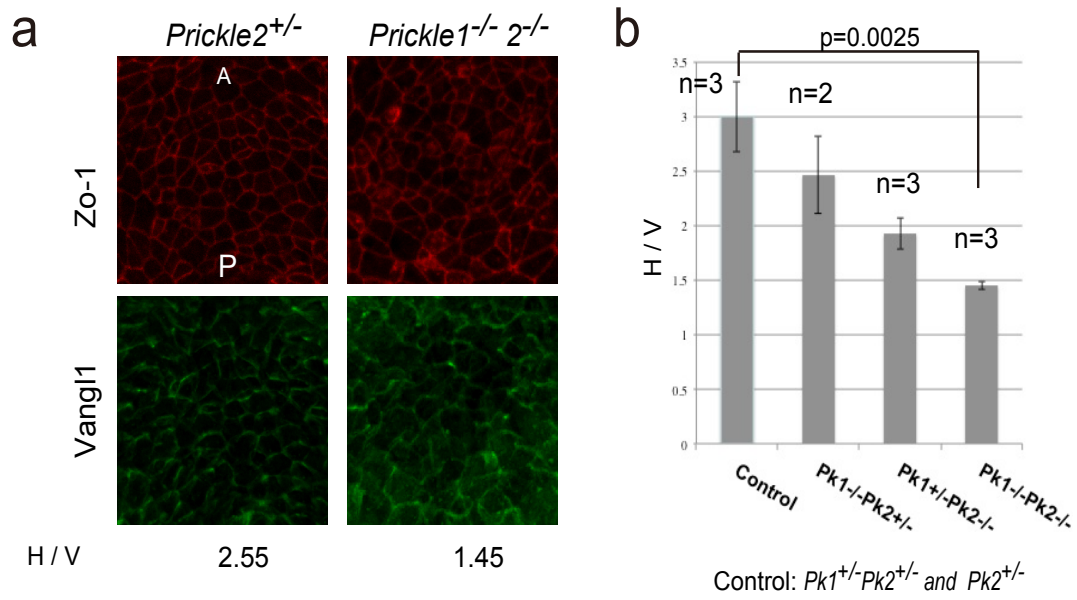

Figure 6. Prickle 1 and 2 are involved in the localization of Vangl1 in node cells

(a) Immunostaining of Zo-1 (red) and Vabgl1 (green) in the control and *Prickle1*$^{-/-}$*2*$^{-/-}$ node at 3-5 So stages. Quantified result (H/V) is shown under each image. **(b)** H/V is significantly reduced in *Prickle1*$^{-/-}$*2*$^{-/-}$ (n=3) as compared to control node (n=3) at 3~5So stage (two-tail t test, p = 0.0025).
Pk, Prickle.

Posteriorly-expressed Wnt5a and Wnt5b are required to polarize node cells

It has been established that the PCP core proteins such as Dvl (Hashimoto et al., 2010) and Vangl (Song et al., 2010) control the positioning of the basal body in node cells of the mouse embryo. However, it is unknown what polarizes node cells and how the polarized distribution of core PCP proteins is established in node cells. To address this, we examined both Wnt-independent and Wnt-dependent mechanisms.

We first investigated the involvement of an Wnt-dependent mechanism. Recent studies have shown the involvement of noncanonical Wnt-regulated PCP in various developmental aspects: Wnt11 in convergent-extension during gastrulation (Heisenberg

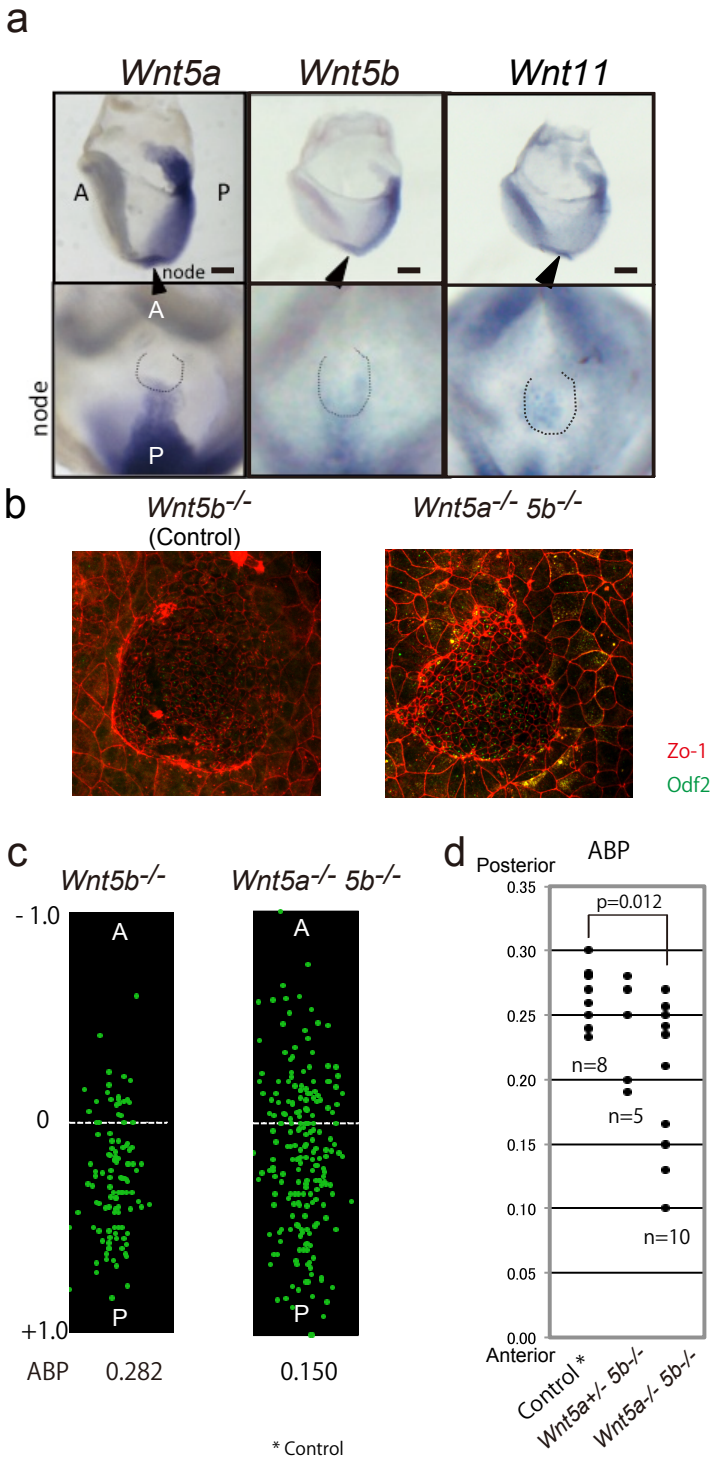

Figure 7. Wnt5a and Wnt5b are required for the positioning of basal body.

(a) Whole-mount in situ hybridization analysis of *Wnt5a*, *Wnt5b* and *Wnt11* at E7.5. The dotted lines indicate the node position. Scale bars: 100 μ m. **(b)** Immunostaining of Zo-1 (red) and Odf2 (green) in the *Wnt5b*$^{-/-}$ (Control) and *Wnt5a*$^{-/-}$*5b*$^{-/-}$ node at 3-5 So stages. **(c)** Relative position of the basal body (green dots) in node of *Wnt5b*-/- (Control) and *Wnt5a*$^{-/-}$*5b*$^{-/-}$ at 3~5 So stage. Corresponding ABP rate is shown under each panel. **(d)** ABP rate is reduced in *Wnt5a*$^{-/-}$*5b*$^{-/-}$ (n=10) versus control (n=8) in node at 3~5 So stages (two-tail t test, p = 0.012). A, anterior; P, posterior.

* Control

WT, Wnt5a+/- , Wnt5b+/-, Wnt5b-/- and Wnt5a+/-;Wnt5b+/-

et al., 2000), Wnt5a in inner ear formation (Qian et al., 2007) and limb patterning (Gao et al., 2011). At least three noncanonical Wnt genes: *Wnt5a*, *Wnt5b* and *Wnt11*, are ectopically expressed in the node and surrounding tissues. While *Wnt11* is expressed uniformly in the node (Fig7 a), *Wnt5a* and *Wnt5b* are expressed in the posterior end of the node and the primitive streak (Fig 7 a). This expression might generate asymmetric distribution of Wnt ligand along the A–P axis. Mutant mice lacking either of these Wnt genes do not show left–right defects. We examined the position of the basal body in node cells lacking *Wnt5a* and *Wnt5b*. *Wnt5a*+/-, *Wnt5b*-/- and *Wnt5a*+/-; *Wnt5b*+/- did not show ABP differences with WT (data not shown). So theses mutants were included in the control group. The ABP was significantly decreased about a half of $Wnt5a^{-/-}$ $Wnt5b^{-/-}$ embryos (5/10 embryos) compared to the control (Fig 7 b, c, d), suggesting that the basal body failed to shift posteriorly.

To test whether Wnt ligands are required for the polarized localization of PCP core proteins in node cells, we examined the localization of Vangl1, which is known to reside on the anterior side of node cells (Fig 5 a) (Song et al., 2010). The H/V ratio of Vangl1 localization was reduced in $Wnt5a^{-/-}$ $5b^{-/-}$ embryos (Fig8 a, b), indicating that the polarized distribution of Vangl1 is impaired in the absence of Wnt5a and Wnt5b. These findings suggested that Wnt5a and Wnt5b are required for the correct basal body positioning by inducing polarized localization of PCP core proteins.

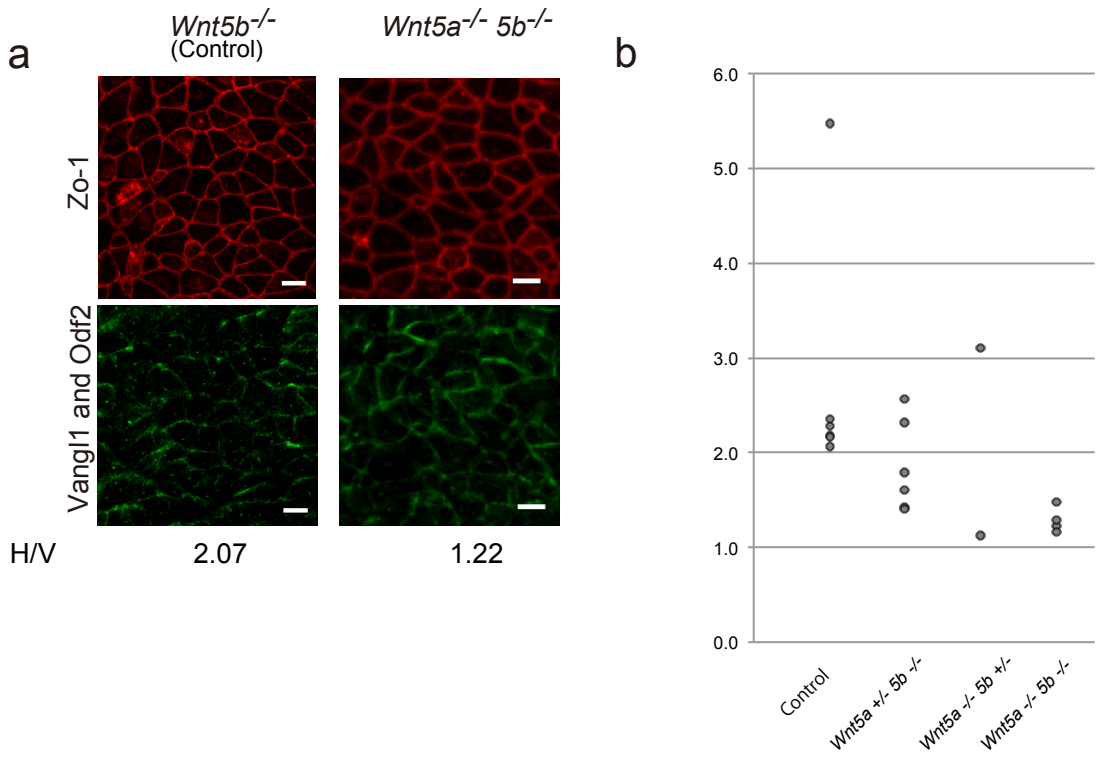

Figure 8. Polarized distribution of PCP core protein is impaired in the absence of Wnt5a and Wnt5b
(a) Immunostaining of Zo-1 (red), Vangl1 and Odf2 (green) in the control and *Wnt5a*$^{-/-}$ *5b*$^{-/-}$ node at 3-5 So stages. Scale bars:5 μ m. Quantified result (H/V) is shown under each image. **(b)** H/V is reduced in the node of *Wnt5a*$^{-/-}$*5b*$^{-/-}$ (n= 4) as compared to control (n= 5).

Sfrps, anteriorly-expressed Wnt inhibitors, also serve as polarizing signals

The position of the basal body was affected by the lack of Wnt5a/5b, but it was so only in a half of the corresponding embryos. These results suggest the presence of additional genes that can contribute to A-P asymmetric distribution of Wnt activity. Plausible candidates were the secreted Frizzled-related proteins (Sfrp) that contain a cysteine-rich domain (CRD) with homology to the Wnt binding domain of Fzd and act as antagonists of Wnt/ β -catenin and PCP pathways (Cruciat and Niehrs, 2013; Satoh et al., 2008). Sfrp1, 2 and 5 are expressed in the developing mouse embryo (Matsuyama et al., 2009).

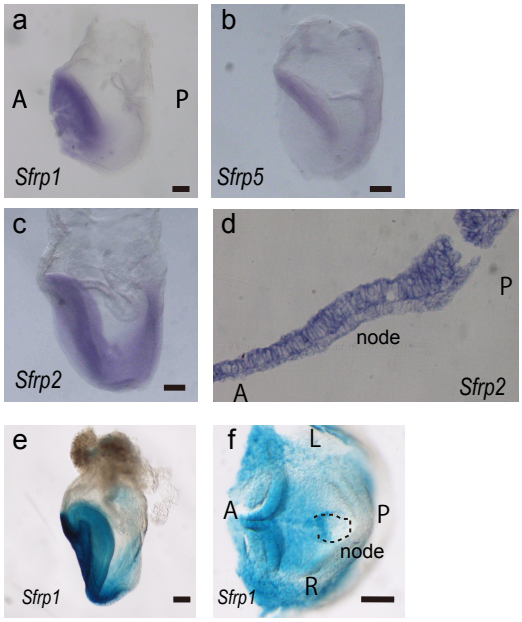

Figure 9. Sfrps are expressed in the anterior region of embryo

Whole-mount in situ hybridization analysis of (a) *Sfrp1*, (b) *Sfrp5* and (c) *Sfrp2* at E7.5. (d) Sagittal section in situ hybridization of Sfrp2 at E7.5. (e) X-gal staining of *Sfrp1*-HA-lacZ/BAC embryos. (f) The image focused on the node of embryo shown in (e). Scale bars: 100 μ m. A, anterior; P, posterior; R, right; L, left.

Interestingly, *Sfrp1* and *sfrp5* are expressed in the region anterior to the node, the opposite side of the *Wnt5a/5b*-expressing domain (Fig. 9 a, b, e, f). Moreover, the expression of Sfrp1 was gradually reduced along A-P axis in contrast with the Wnt5a/5b expression pattern (Fig 9 a). Sfrp2 was widely expressed in the embryo, but its expression was gradually reduced along A-P axis in the node (Fig 9 c d). Therefore, we hypothesized that Sfrps reinforce the polarized Wnt signals in or near the node.

To test this hypothesis, we examined the basal body position and the localization of Vangl1 in node cells in Sfrp mutant embryos, and found that the lack of

Figure 10. Sfrps are involved in the polarization of node cells

(a) Immunostaining of Zo-1 (red) and Odf2 (green) in the node of WT and *Sfrp1*$^{-/-}$*2*$^{-/-}$*5*$^{-/-}$ at 3-5 So stage. **(b)** A-P relative position of the basal body (green dots) in node of WT and *Sfrp1*$^{-/-}$*2*$^{-/-}$*5*$^{-/-}$ at 3-5 So stage. Quantified result (ABP) is shown under each image. **(c)** ABP rate is reduced in *Sfrp1*$^{-/-}$*2*$^{+/-}$*5*$^{-/-}$ (n=8) and *Sfrp1*$^{-/-}$*2*$^{-/-}$*5*$^{-/-}$ (n=3) node compared to control (n=8) at 3-5 So stage. (two-tail t test, p = 0.004 and 1.62×10^{-8}). **(d)** Immunostaining of Zo-1 (red) and Vangl1 (green) in the node of WT and *Sfrp1*$^{-/-}$*2*$^{-/-}$*5*$^{-/-}$ at 3-5 So stage. Quantified result (H/V) is shown under each image. **(e)** Immunostaining of Zo-1, Odf2 and Celsr1 in the WT and *Sfrp1*$^{-/-}$*2*$^{-/-}$*5*$^{-/-}$ node at 3-5 So stages. High panel: Zo-1(red) and Odf2 (green), Middle panel: Zo-1 (red) and Celsr1 (green), Low panel: Odf2 (red) and Celsr1 (green). Scale bars: 10 μ m. A, anterior; P, posterior.

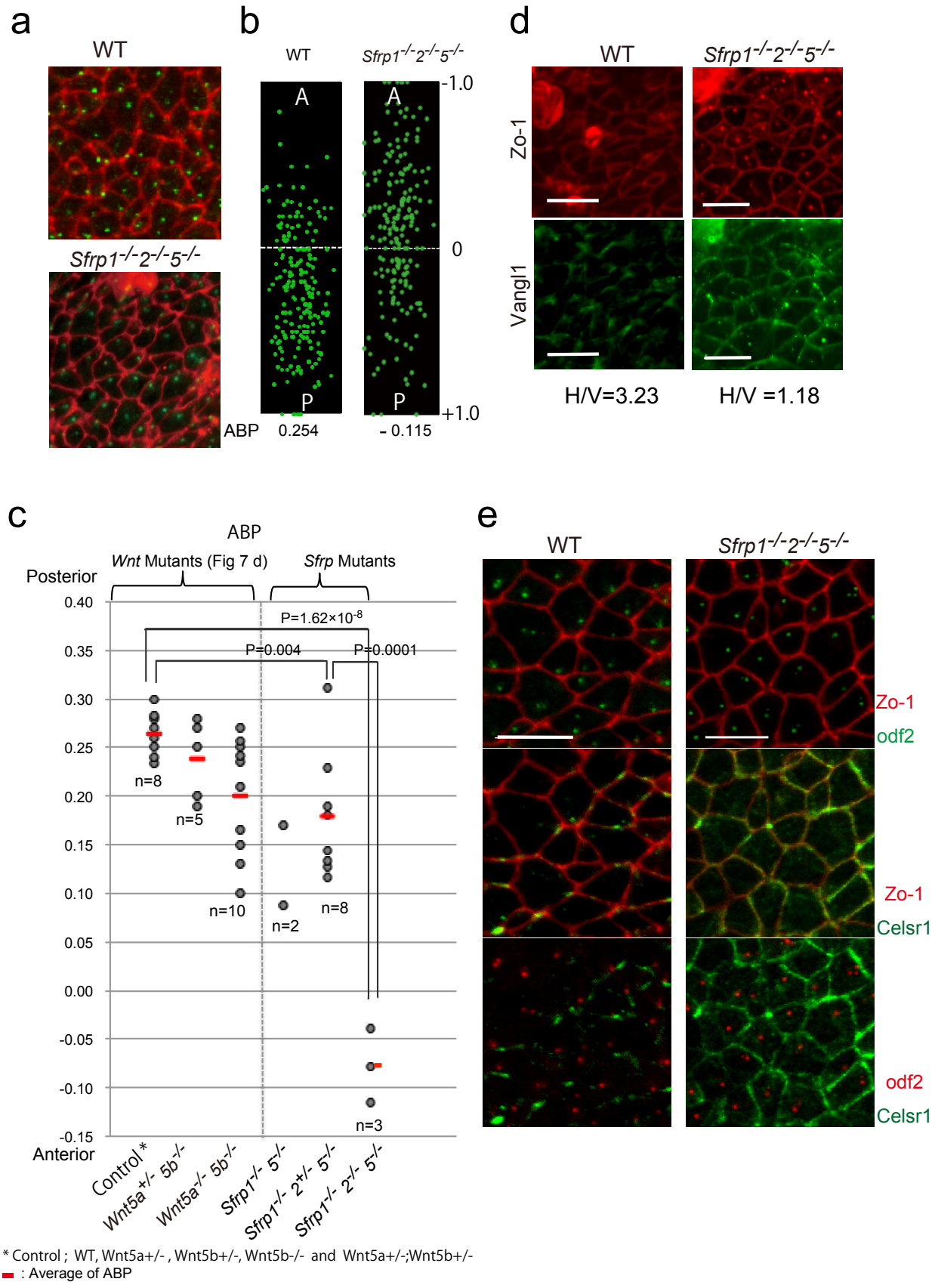

these Sfrps have similar yet more profound effects on node cell polarization than the

lack of Wnt5a and Wnt5b. Thus, in the *Sfrp1*$^{-/-}$*2*$^{+/-}$*5*$^{-/-}$ (4/8) and *Sfrp1*$^{-/-}$*2*$^{-/-}$*5*$^{-/-}$ (3/3) embryos examined, the basal body position was impaired (Fig 10 a, b, c). PCP core proteins such as Vangl1 and Celsr1 were randomly localized on the membrane of node cells in the *Sfrp1*$^{-/-}$*2*$^{-/-}$*5*$^{-/-}$ embryos (Fig 10 d, e). These results suggest that polarization of node cells requires these Sfrps.

Furthermore, to test whether the asymmetric distribution of Sfrps along the A–P axis is required to polarize node cells, we cultured the embryos with recombinant Sfrp1 starting from the late streak stage, right before the posterior shift of the basal body. Treatment of the WT embryos with recombinant Sfrp1 significantly reduces the ABP (Fig 11 a, b), suggesting that uniform distribution of Sfrp1 protein impairs the basal

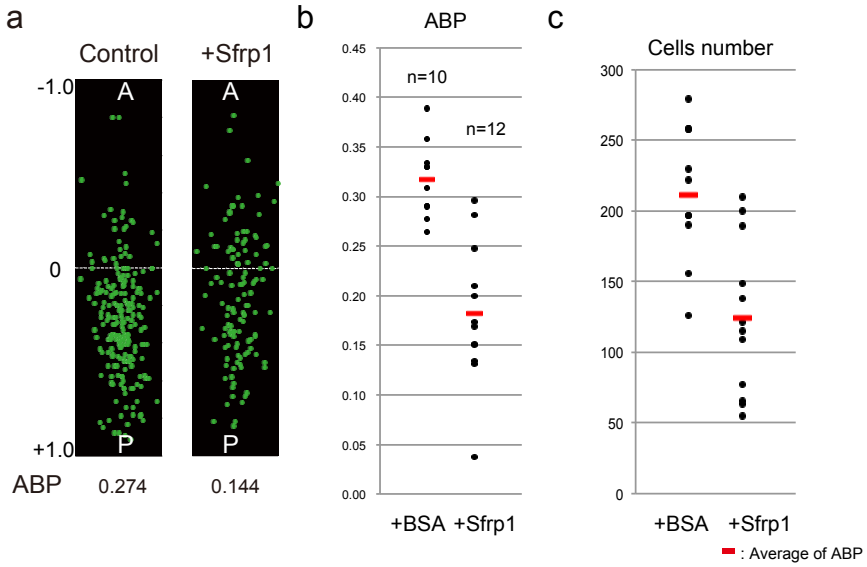

Figure 11. Uniform distribution of Sfrp1 protein impairs the basal body positioning in node cells
Embryos were cultured with BSA as control condition or with recombinant Sfrp1 starting from the late streak stage to 3-5 So stage. **(a)** A-P relative position of the basal body (green dots) in node with BSA or with recombinant Sfrp1. Corresponding ABP is indicated under each panel. **(b)** The ABP is reduced in embryos with Sfrp1 (n=12) compared to control (n=10). **(c)** The number of cells in the node after culture. A, anterior P, posterior. The red bar indicates the average of ABP.

body positioning in node cells. The number of cells was also reduced in the node

cultured with recombinant Sfrp1 (Fig 11 c).

Uniform expression of Wnt5a/5b impairs polarization of node cells

The phenotype of the *Wnt5a*$^{-/-}$ *5b*$^{-/-}$ embryo does not distinguish whether Wnt5a and Wnt5b act as permissively or instructively for basal body positioning. To clarify the importance of the asymmetric distribution of Wnt ligand along the A–P axis, we induced uniform expression of Wnt5a in whole embryos. We tested whether the exogenously added Wnt5a impairs the basal body positioning in node cells. We cultured embryos with recombinant Wnt5a starting from late streak stage, when the basal body is localized in a relatively central region in node cells, and evaluated the posterior positioning of the basal body at three-somite stage. Compared to control conditions, treatment with recombinant Wnt5a significantly reduces the ABP, although the node's morphology remained normal (Fig 12 a, b, Fig 13 c). These results indicated that the exogenous and uniform Wnt5a protein affected the basal body position in node cells. Furthermore, *Wnt5a-/- 5b-/-* embryos cultured with recombinant Wnt5a did not rescue the defect of basal body positioning (Fig 12 c), raising the possibility that uniformly Wnt5a presence is not enough to make a rescue.

To induce uniformly Wnt5a expression, we used transgenic mice with overexpression of Wnt5a (*Rosa*$^{Wnt5a/+}$ *Sox2-Cre*) (Cha et al., 2014) and then confirmed that the expression pattern was uniform in the embryo (Fig 13 a).

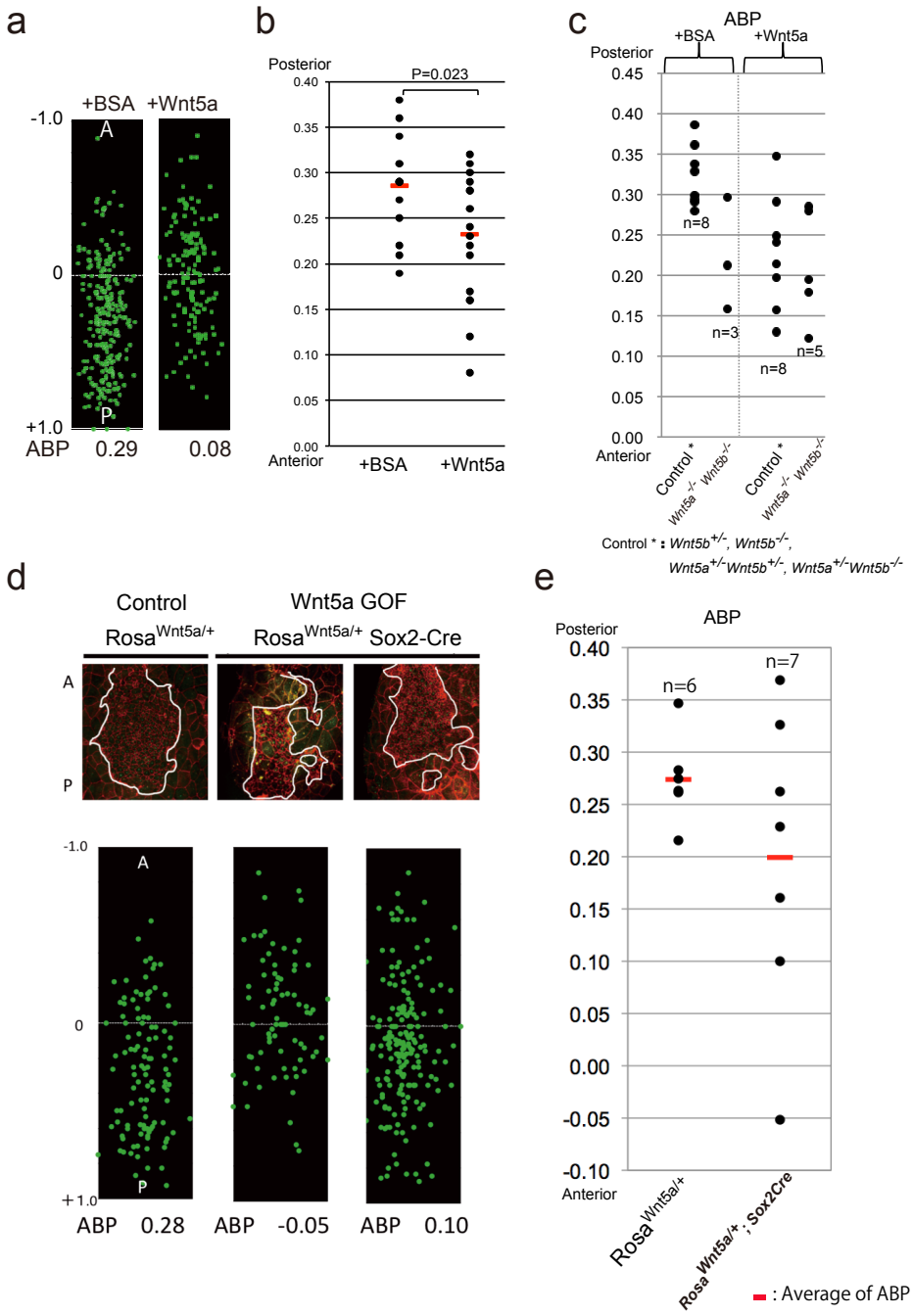

Figure 12. Exogenous and uniform Wnt5a protein affects the basal body position in node cells.

(a)-(b) Embryos were cultured with BSA (control) or recombinant Wnt5a starting from the late streak stage to 3-5 So stage. **(a)** A-P relative position of the basal body (green dots) in node. **(b)** The ABP is reduced in embryos with Wnt5a (n=19) compared to control (n=14) (two-tail t test, p =0.023). **(c)** *Wnt5a*$^{-/-}$ *5b*$^{-/-}$ embryos were cultured with BSA or with recombinant Wnt5a. The ABP is reduced in *Wnt5a*$^{-/-}$*5b*$^{-/-}$ compared to control in both condition: with BSA and with recombinant Wnt5a. *Wnt5a*$^{-/-}$ *5b*$^{-/-}$ embryos cultured with recombinant Wnt5a did not rescue the defect of basal body positioning. **(d)-(f)** Uniform Wnt5a expression was induced by the transgenic mice with overexpression of Wnt5a (*Rosa*$^{Wnt5a/+}$ *Sox2-Cre*). **(d)** Images were taken by the immunostaining of Zo-1 (red) and Odf2 (green) in *Rosa*$^{Wnt5a/+}$ (control) and *Rosa*$^{Wnt5a/+}$ Sox2-Cre node at 3-5So stage. The white line indicates the shape of node. The corresponding relative position of the basal body (green dots) in node and the ABP values are indicated under each image. (e) The ABP is reduced in *Rosa*$^{Wnt5a/+}$ *Sox2-Cre* node compared to control. The red bar indicates the average of ABP. A, anterior; P, posterior.

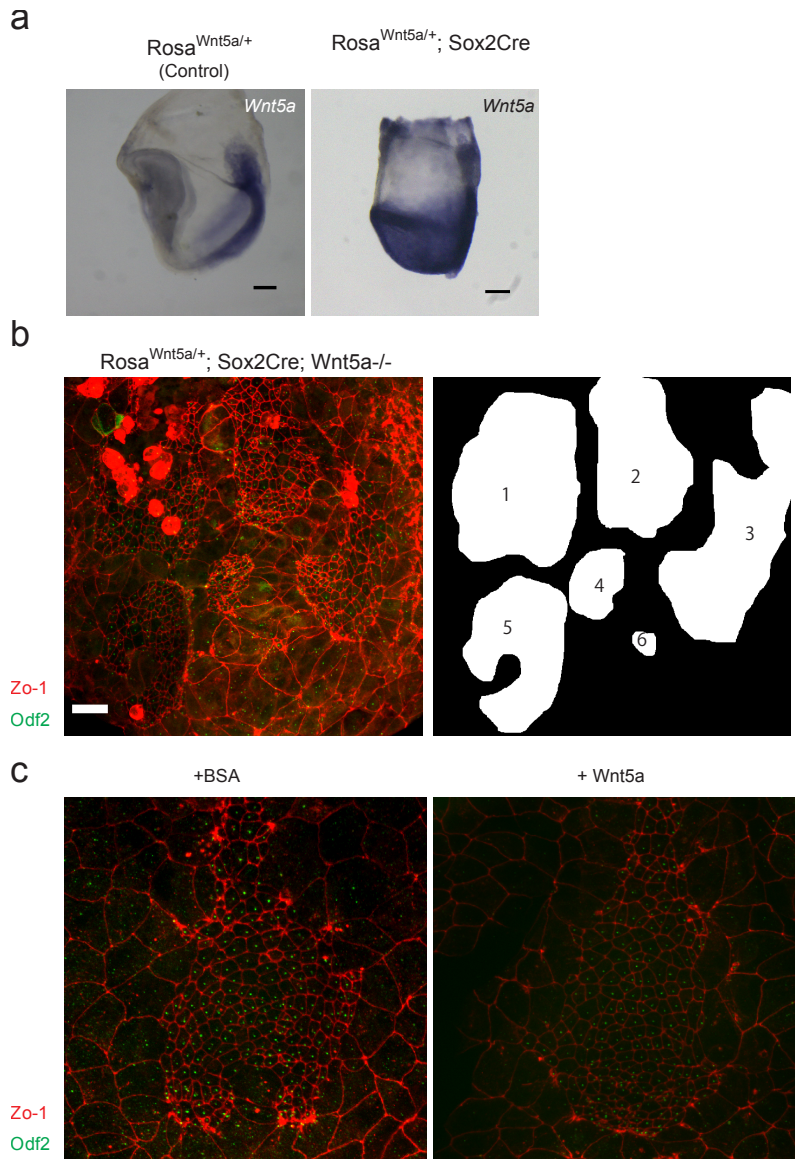

Figure 13. Transgenic mice with overexpression of Wnt5a (*Rosa*$^{Wnt5a/+}$*; Sox2-Cre*)

(a) Whole-mount in situ hybridization analysis of Wnt5a in *Rosa*$^{Wnt5a/+}$ (control) and *Rosa*$^{Wnt5a/+}$; *Sox2-Cre* embryos at E7.5. Scale bars:100 μ m. **(b)** Node of *Wnt5a*$^{-/-}$ *5b*$^{-/-}$ *;Rosa*$^{Wnt5a/+}$; Sox2-Cre embryos have multiple fragmented node pieces . Left panel: Immunostaining of Zo-1 (red) and Odf2 (green). Scale bars:20 μ m. Right panel: Schematic representation of the corresponding six fragmented node areas. **(c)** Morphology of 3-5 So stage embryo's node cultured with recombinant Wnt5a remained normal.

Several embryos were found to have irregular shapes or fragmented node (Fig 12 d). Wide variation of ABP in *Rosa*$^{Wnt5a/+}$ *Sox2-Cre* was noticed and some embryos showed a decreased ABP (Fig 12 d, e). These data implied that uniformly Wnt5a expression impaired the formation of the node and a posteriorly-shifted basal body. Furthermore, node of Wnt5a-/- 5b-/- mice overexpressing Wnt5a (*Rosa*$^{Wnt5a/+}$ *Sox2-Cre Wnt5a*$^{-/-}$ *5b*$^{-/-}$) showed multiple fragmented node pieces (Fig 13 b). This abnormal node formation may be a consequence of impaired gastrulation.

Thus the uniform Wnt5a expression and the mutant embryos lacking Wnt5a and Wnt5b showed the same defect of basal body positioning. These findings supported the importance of asymmetric distribution of Wnt ligand along the A–P axis for the polarization of node cells.

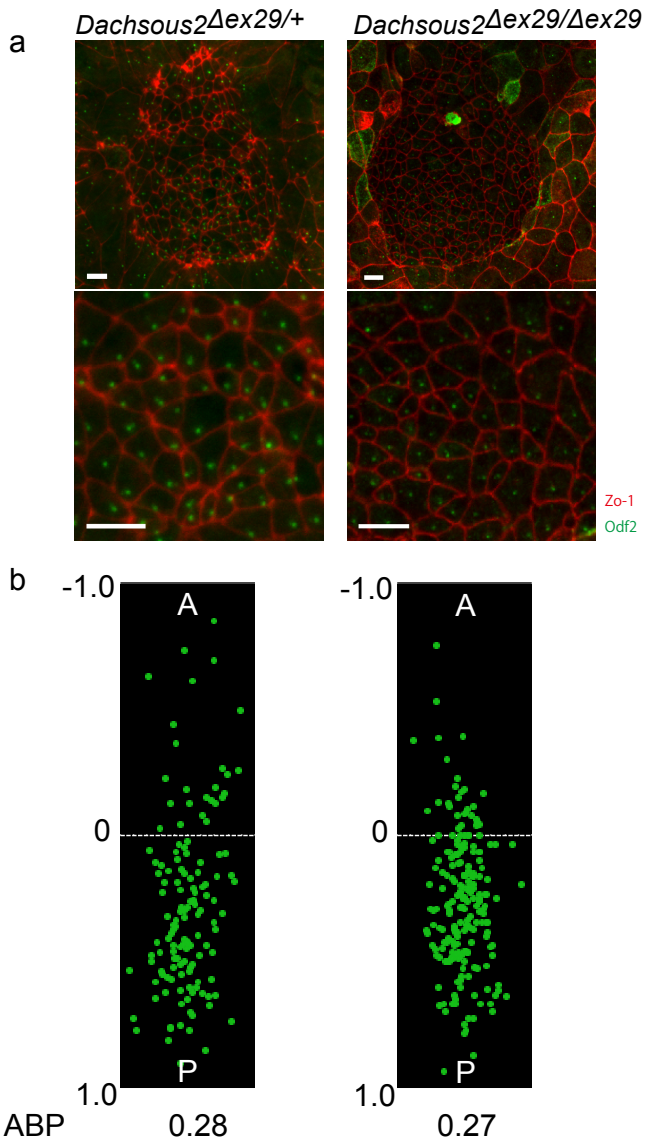

Figure 14. The posterior positioning of the basal body is normally determined in the Dachsous2 $^{\Delta wx29/\Delta ex29}$ node.
(a) Immunostaining of Zo-1 (red) and Odf2 (green) in the node of Dachsous2 $^{\Delta ex29/+}$ and Dachsous2 $^{\Delta wx29/\Delta ex29}$ at 3-5 So stage. Higher magnification is shown in the lower panel. **(b)** A-P relative position of the basal body (green dots) in node of Dachsous2 $^{\Delta ex29/+}$ and Dachsous2 $^{\Delta wx29/\Delta ex29}$ at 3-5 So stage. Quantified result (ABP) is shown under each image. Scale bars: 10 μ m. A,

Are Dacshous2 required for the polarization of node cells?

In Drosophila, Wnt ligands do not seem to play direct role in regulating the PCP pathway. Instead, the global polarity cue is considered to be generated by a local cell-cell interaction involving “Four-jointed” and two protocadherins “Fat” and “Dachsous” (Matakatsu and Blair, 2004; Villano and Katz, 1995). Mutant mice lacking Dachsous1 protein do not show L-R defects (Mao et al., 2011). In mammals, two types of Dachsous have been identified: Dachsous1 and Dachsous2. A functional redundancy is possible between these two proteins. To examine whether Dachsous is required to polarize node cells, we generated Dachsous2 mutant mice lacking exon 29 by a conventional ES cell-mediated targeting (Fig. S1). *Dachsous2* $^{\Delta wx29/\Delta ex29-}$ mice are viable and fertile, and showed no obvious morphological defects. The ABP value was not affected in the node of Dachsous2 $^{\Delta wx29/\Delta ex29}$ (Fig14 a, b).

DISCUSSION

Whereas it was clear that the PCP signaling system controls the positioning of the basal body in node cells, it was unclear how initial global A-P axis regulates the polarized distribution of core PCP proteins. Our study showed that the polarization of node cells is determined by a combination of the posteriorly-expressed Wnt5a/5b and anteriorly-expressed Wnt antagonists Sfrps.

How Dose initial global A-P axis regulate the polarized distribution of core PCP proteins in node cells?

Previous studies have shown that several noncanonical Wnt proteins regulate PCP in various developmental aspects (Gao et al., 2011; Heisenberg et al., 2000; Qian et al., 2007). However, in the node, PCP regulation by Wnts has not been established, since mutant mice lacking either of Wnt5a or Wnt5b did not show L-R defects (Majumdar et al., 2003; Yamaguchi et al., 1999). Based on double mutant studies, we have demonstrated, for the first time, that both Wnt5a and Wnt5b control PCP in the node. Surprisingly, we found that Sfrp proteins were also involved and required for node cells polarization. From our results, we anticipate that the initial global A-P in the node is defined by a combination of the posteriorly-expressed Wnt5a/5b and anteriorly-expressed Sfrps. This global A-P information is translated into local areas. This determines the node cell polarization and finally leads to the establishment of L-R patterning (Fig15 model). Our model was supported by the fact that Sfrp1 can interact with Wnt5a in vitro (Matsuyama et al., 2009). The uniform Wnt5a expression and mutant embryos lacking Wnt5a and Wnt5b showed the same basal body positioning

defect, suggesting a possibility that the asymmetric distribution of Wnts and Sfrps is required for the basal body positioning. However, having embryos expressing a reversed distribution of Wnt ligand would provide a direct evidence.

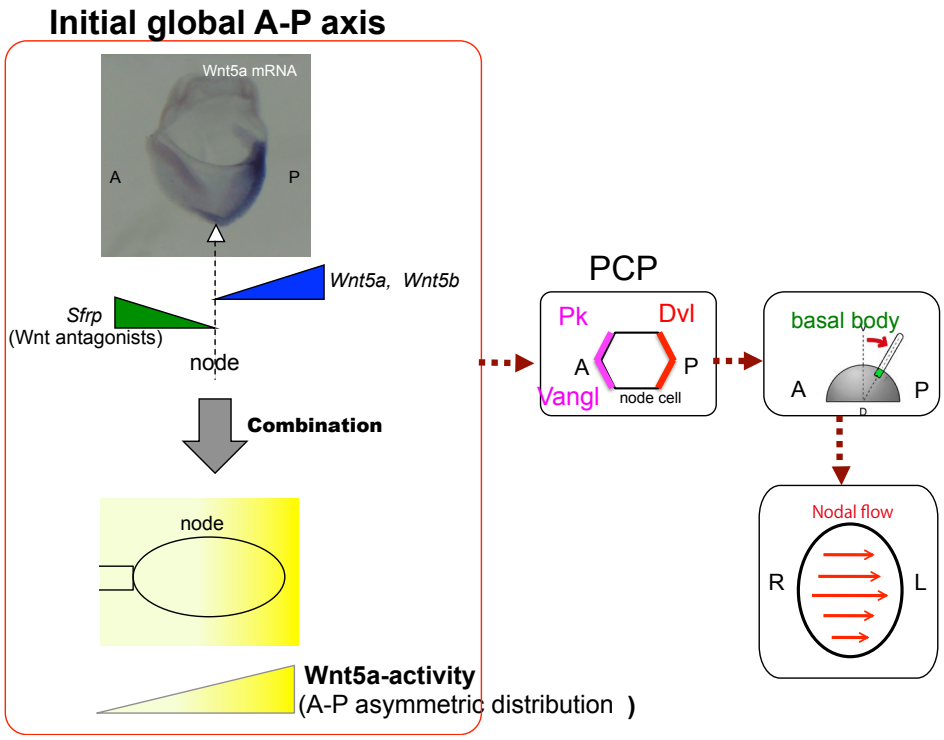

Figure 15. Model of polarization of the mouse node cells by asymmetric distribution of Wnt5a/5b and their inhibitors

A combination of the posteriorly-expressed Wnt5a/5b and anteriorly-expressed Wnt antagonists (Sfrps) might generate the A-P asymmetric distribution of Wnt5a activity.

Thus, giving birth to the initial cues of PCP pathway regulation, namely, the global A-P axis signals. Subsequently, at node cell level, the global signals are translated into local areas: Pk and Vangl on the anterior side versus Dvl on the posterior side. This leads to the posterior localization of the basal body, the generation of Nodal flow and finally the establishment of L-R patterning. A; anterior , P; posterior, R; Right, L; Left.

Prickle is required for basal body positioning and support the distribution of Vangl in node cells

We found that Prickle proteins play the same role as Vangl and Dvl in the basal body positioning. Moreover, our result showed aberrant distribution of Vangl1 in *Prickle1*$^{\Delta ex6/\Delta ex6}$ *Prickle2* $^{\Delta ex6/\Delta ex6}$ node cells. Other reports indicated that Prickle protein can interact with Vangl in vitro (Bastock et al., 2003) and we revealed that Prickle2 and Vangl1 are localized at the anterior end of node cells (Fig 5 a, b). These observations suggest an intriguing possibility that the anteriorly localized Vangl1 is amplified by its interaction with Prickle in node cells.

Are Dachsous involved in the polarization of node cells?

In Drosophila, Dachsous and Fat proteins function as ligand and receptor, respectively for the PCP (Matakatsu and Blair, 2004). Recent studies have shown that Dachsous and Fat families play a role in vertebrate planar polarity (Mao et al., 2011; Saburi et al., 2008). In this report, the posterior positioning of the basal body is normally determined in the *Dachsous2* $^{\Delta wx29/\Delta ex29}$ node. *Dachsous2* $^{\Delta wx29/\Delta ex29}$ did not show left–right defects. However, to clear the role of Dachsous family in node cell polarity, it is necessary to examine the basal body position in *Dchs1*$^{-/-}$ *Dachs2*$^{-/-}$ node cells.

Previous repots showed involvement of Wnt family in the regulation of PCP pathway in diverse developmental processes. We propose a mechanism where this regulation happens from a combination of the Wnts and Wnt antagonists (Sfrps), rising the possibility that the same mechanism may occur in other tissues and species.

MATERIALS AND METHODS

Mice

Rosa$^{Wnt5a/+}$ mice, *Sox2-Cre* mice and all Wnt5a, Wnt5b, Wnt11, Sfrp1, Sfrp2 and Sfrp5 mutant mice were previously described (Agalliu et al., 2009; Cha et al., 2014; Hayashi et al., 2002; Majumdar et al., 2003; Satoh et al., 2006; Satoh et al., 2008; Yamaguchi et al., 1999).

Prickle1$^{\Delta exon6/+}$, *Prickle2*$^{\Delta exon6/+}$ and *Dchs2*$^{\Delta exon29/+}$ were generated by conventional ES cell-mediated targeting (Fig. S1). Each specific primer sets were used for detection of the WT allele and deleted allele (Fig. S1). Prickle1 primer set for WT allele is Pk1-WT-F (aatcggcgaatgccaatg) and Pk1-WT- R (ggatttcatccctaacacaccac). *Prickle1* primer set for Δ ex6 allele is Pk1-Mut-F (gtgactgcaaacaagcgaaa) and Pk1-Mut-R (gcattgacttgccaccagta). *Prickle2* primer set for WT allele is Pk2-WT-F (cacatacatgcacacccacaattc) and Pk2-WT-R (tcagggttgttttcaacttcaaagc). *Prickle2* primer set for Δ ex6 allele is Pk2-WT-F and Pk2-Mut-R (ggcctctatggaagggaaag). *Dachsous2* primer set for WT allele is Ds2-WT-F (cttgatgtaaggctgcgatg) and Ds2-WT-R (caaacttcaaaagtggacattgag). *Dachsous2* primer set for Δ ex29 allele is Ds2-Mut-F (ggtggggcacaatctagaaa) and Ds2-WT-R.

Sfrp1-BAC HA-Tag Ires LacZ transgene was produced from the Sfrp1 BAC with a HA-Tag –Iles LacZ at the Cterminal of Sfrp1 CDS.

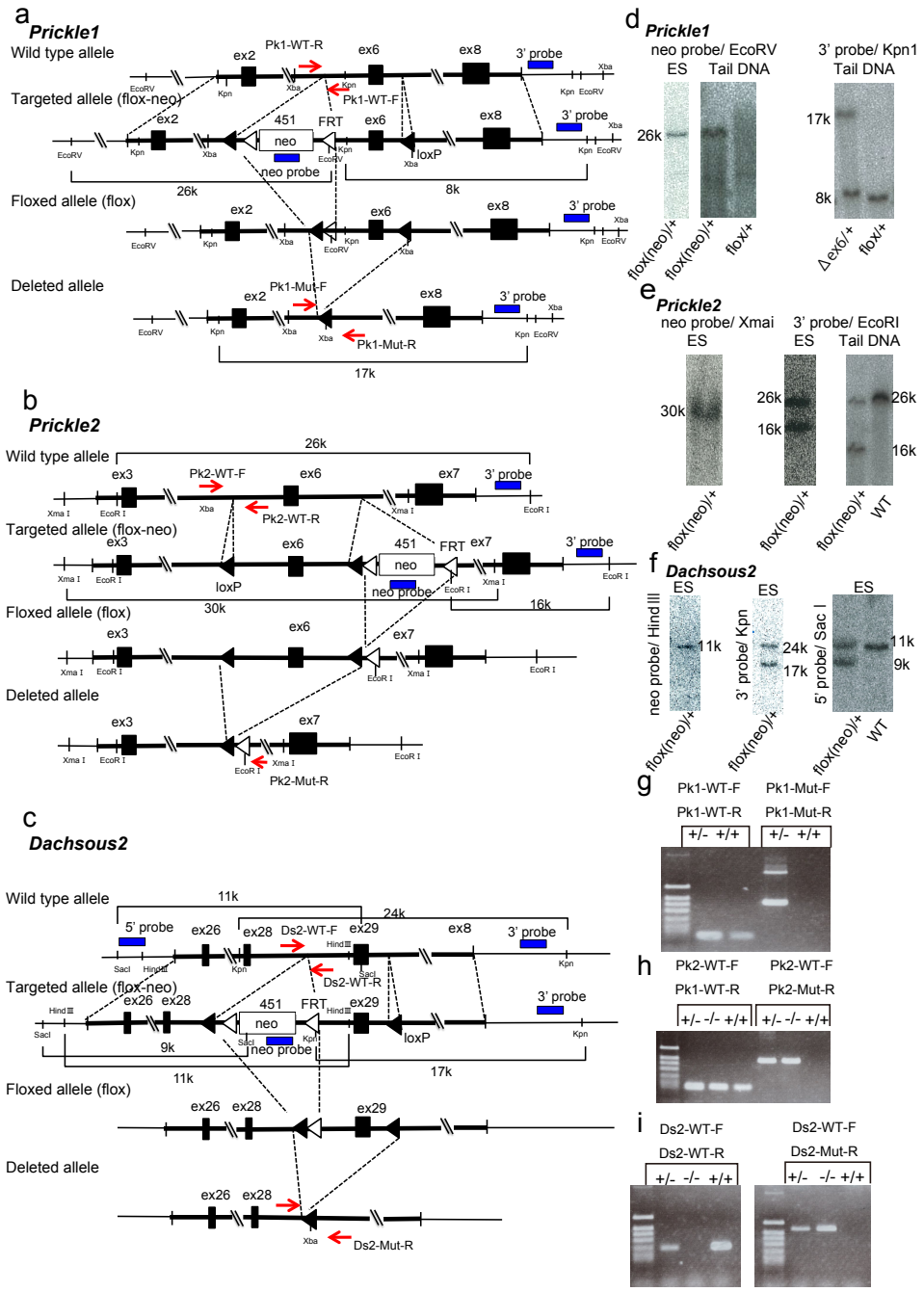

Figure S1 ***Prickle1, Pricke2*** **and** ***Dachsous2*** **knockout targeting mice**

(a), (b), (c) To generate each *Prickle1, Prickle2 and Dachsous*2 knockout targeting vectors, a cassette consisting of Frt-Pgk-em7-neo-Frt-LoxP from the PL451 vector was inserted into (a) upstream of *Prickle1* exon6, (b) downstream of *Prickle2* exon6 and (c) upstream of *Dacshous2* exon29. And then a single LoxP site was inserted into (a) downstream of *Prickle1* exon6, (b) upstream of *Prickle2* exon6 and (c) downstream of *Dachsous2* exon29. The targeted exon and the neo cassette were removed by the CAG-Cre or CAG-flp transgenic mice. Red arrow, primer for PCR; Blue bar, probe for Southern blot hybridization. **(d), (e), (f)** The homologous recombinants were detected by Southern blot hybridization with a series of specific probes that target external or internal sites relative to the vector sequence. **(g), (h), (i)** PCR analyses of tail DNA from offspring obtained from the heterozygous intercross. Specific primer sets were used for detection of the WT allele and null allele. Prickle1 Δex6/+, Pk1 +/-; Prickle2 Δex6/+, Pk2+/-; Dachsous2 Δex29/+, Ds2+/-.

Whole-mount in situ hybridization and X-gal staining

Whole-mount in situ hybridization was performed according to standard protocols with specific RNA probes for each Wnt5a, Wnt5b, Wnt11, Prickle1, Prickle2, Sfrp1, Sfrp2 and Sfrp5.

Gifted plasmids :

Sfrp1, Sfrp2, Sfrp5 (gifted by Dr A. Shimono, (Satoh et al., 2008)), Prickle1 (gifted by Dr N. Ueno and Dr H.Tao), Wnt5a and Wnt5b (gifted by Dr AP. McMahon).

Plasmids produced by TA Cloning :

Each specific sequences were amplified from embryonic gDNA (E12.5) using the following primers: Prickle2, caactcctcaatgcagttcagg and gccaggtccgacacagtcc; Wnt11, gcagtgacagctgcgacc and cttggagcagcctggaagg. And then the PCR products were cloned into vector using a TA Cloning Kit (Invitrogen).

The LacZ transgenic embryos were stained with X-gal as described previously (Saijoh et al., 1999).

Immunofluorescence analysis

Dissected embryos were fixed in 4% paraformaldehyde, and dehydrated in methanol. 0.1% Triton X-100 in phosphate-buffered saline was used for embryos permeabilization. Primary antibodies and Alexa Fluor-conjugated secondary antibodies were incubated at 4°C overnight.

Primary antibodies included: anti-ZO-1 (mouse, 1:10 dilution; (gifted by Dr S. Tsukita, Osaka University, Japan), anti- Vangl1 (rabbit, 1:250 dilution; Sigma), anti-Odf2 (rabbit,

1:250 dilution; gifted by Dr S. Tsukita,), Anti-Cenexin1/Odf2 (rabbit, 1:250 dilution; abcam) , anti-celar1 (pig, 1:100 dilution; gifted by Dr T. Fujimori, National Institute for Basic Biology, Japan) and anti-prickle2 (rabbit, 1:100 dilution; gifted by Dr T. Ohtsuka, Yamanashi University, Japan).

Fluorescent imaging was performed using FV-1000 confocal microscope (Olympus).

To clarify the precise localization of PCP core protein in a cell, we used the Olympus Super Resolution software (FV-OSR) and a high-sensitivity detector (FV12-HSD) with the FV-1000 confocal microscope.

Whole-embryo culture and recombinant protein treatment

Mice embryos were dissected into phenol red–free Dulbecco's modified Eagle's medium (DMEM) supplemented with 10% fetal bovine serum (Invitrogen). Dissected embryos were transferred in a 50ml tube loosened lid with 75% rat serum/ DMEM and then placed on rotator inside a CO2 incubator (5% CO2, 37℃).

Culture was performed with the recombinant proteins or BSA starting from late streak stage to 3 -5 somite stage. Final concentration: 1.0μg/ml Wnt5a recombinant protein (No.645-WN, R&D Systems) and 200ng/ml Wnt5a recombinant protein (gifted by Dr Karl Willert) or 25.0μg/ml SFRP-1 (No.5396-SF-025, R&D Systems).

Observation of nodal flow and PIV analysis

To observe the nodal flow, we used multi-point scanning confocal microscopy and the Particle Image Velocimetry (PIV) analysis.

Dissected embryos were first cultured under 5% CO2 at 37℃ in phenol

red-free DMEM supplemented with 75% rat serum for about 30min. The region containing the node was then excised and the node cavity was filled with DMEM supplemented with 10% fetal bovine serum and fluorescent microbeads (0.2 μ m in diameter with excitation and emission wavelengths of 505 and 515 nm, respectively (Invitrogen)). The motions of the beads were observed in planes of +5 and +10 μ m relative to the cavity for 10 s (30 frames per s) with the use of CSU-X confocal unit (Yokogawa) and an iXon EMCCD camera (Andor Technology) connected to a DMI6000B microscope (Leica) equipped with a 63× glycerine-immersion objective lens. Time-series images for PIV analysis were captured at a resolution of 512 by 512 pixels and were processed with interrogation windows of 16 by 16 pixels with 50% overlap, corresponding to a spatial resolution of 4.3 by 4.3 μ m. The time-averaged velocity distributions were calculated for 10-s intervals.

Quantitative analysis of basal body position

The average basal body position (ABP) represents the relative position of the basal body in each cell along the A-P axis (vertical) as described previously (Hashimoto et al., 2010).

Improved method of the relative value of the basal body in each cell was measured by ImageJ and MATLAB software as follow.

Confocal images of node immunostaing with Odf2 and Zo-1 determined the position of the basal body and the size of node cells. The region containing the node was initially excised from the confocal images (“node-image”, Fig S2 b).

To characterize the shape and orientation of cells in the node, the outline of each cell

was calculated from Zo-1 staing images using ImageJ software (http://rsb.info.nih.gov/nih-image/) plugin to apply watershed segmentation ("Binary watershed lines-image" Fig S2 c).

To obtain the coordinate data (x,y) of the basal body and cells using MATLAB software, we marked up the dots in the merged images "node-image" and "Binary watershed lines-image" using graphical user interface (GUI) (Fig S2 d). The cells including the marked dot were numbered. The relative value of the basal body in each cell was calculated using these coordinate data. The anterior and posterior ends of a cell are represented by –1.0 and +1.0 respectively (Fig S2 e). The distribution map of the basal body and ABP value were obtained (Fig S2 f).

Y. Igarashi (Olympus Software Technology Corporation) programed this.

Quantification of PCP core protein distribution in the node

Using Vangl1 staining signal, we measured the positive cell borders orientation in reference to the A-P axis. The node region was initially excised from the confocal images showing node immunostained with Vangl1and Zo-1 ("node-image", Fig 3 b). Vangl stained images ("Vangl1-image", Fig S3 c) were processed through binarization using ImageJ software ("binarization-image", Fig S3 d). We traced white lines with "Straight line selections" tool (Fig S3 e, f) and then obtained the angles of each line using ImageJ software (Fig S3 g). The white lines were labeled as horizontal (angle between $0^\circ \sim 45^\circ$, $135^\circ \sim 225^\circ$ and $315^\circ \sim 360^\circ$) or vertical (angle between $45^\circ \sim 135^\circ$ and $225^\circ \sim 315^\circ$) and the proportion between those two populations was estimated by a H/V rate (Fig S3 h).

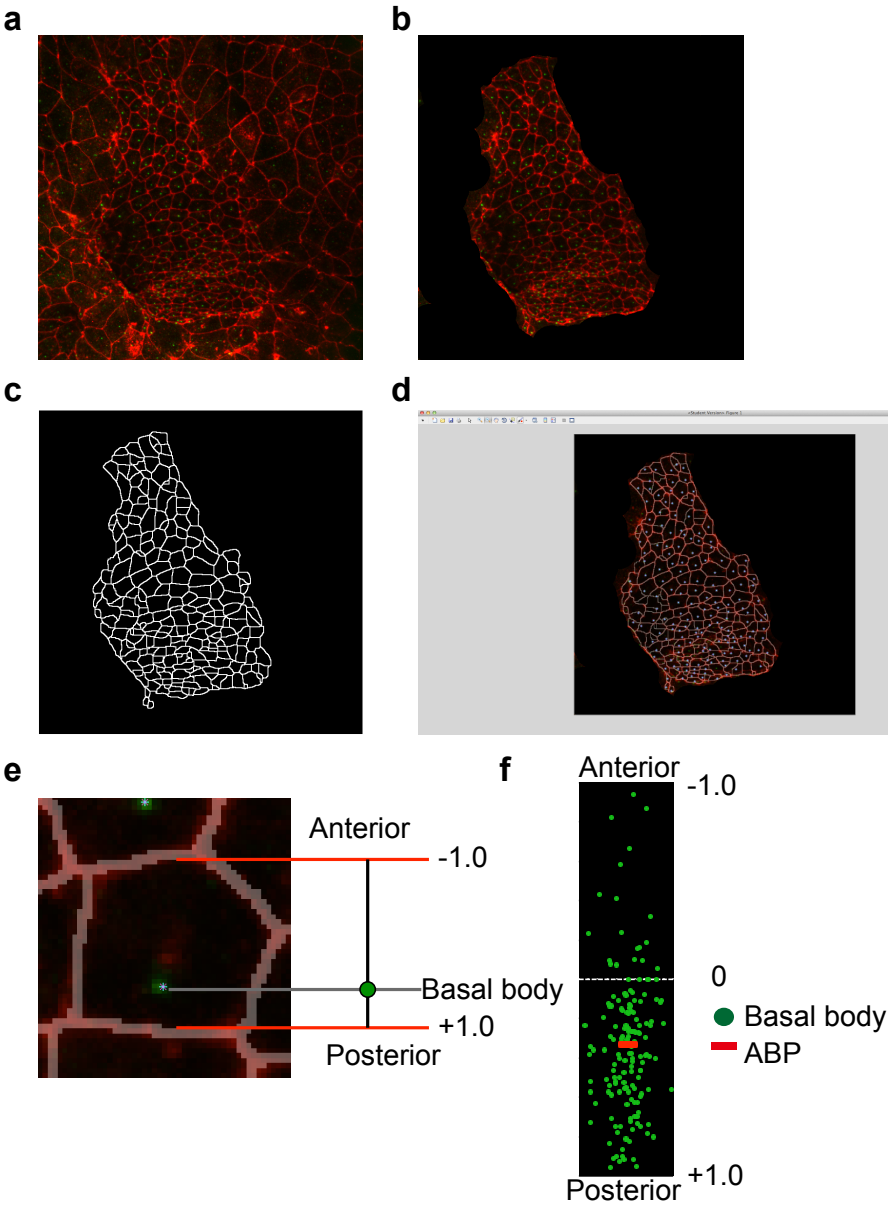

Figure S2 Quantitative analysis of basal body position

(a) Confocal image of the node immunostained for the Odf2 (green) and Zo-1 (red). **(b)** Only node excised from the confocal image, "node-image". **(c)** The ImageJ software plugin to apply watershed segmentation, "Binary watershed lines-image". **(d)** Graphical user interface (GUI). **(e)** Relative value of the basal body. **(f)** Distribution map of basal body and ABP value

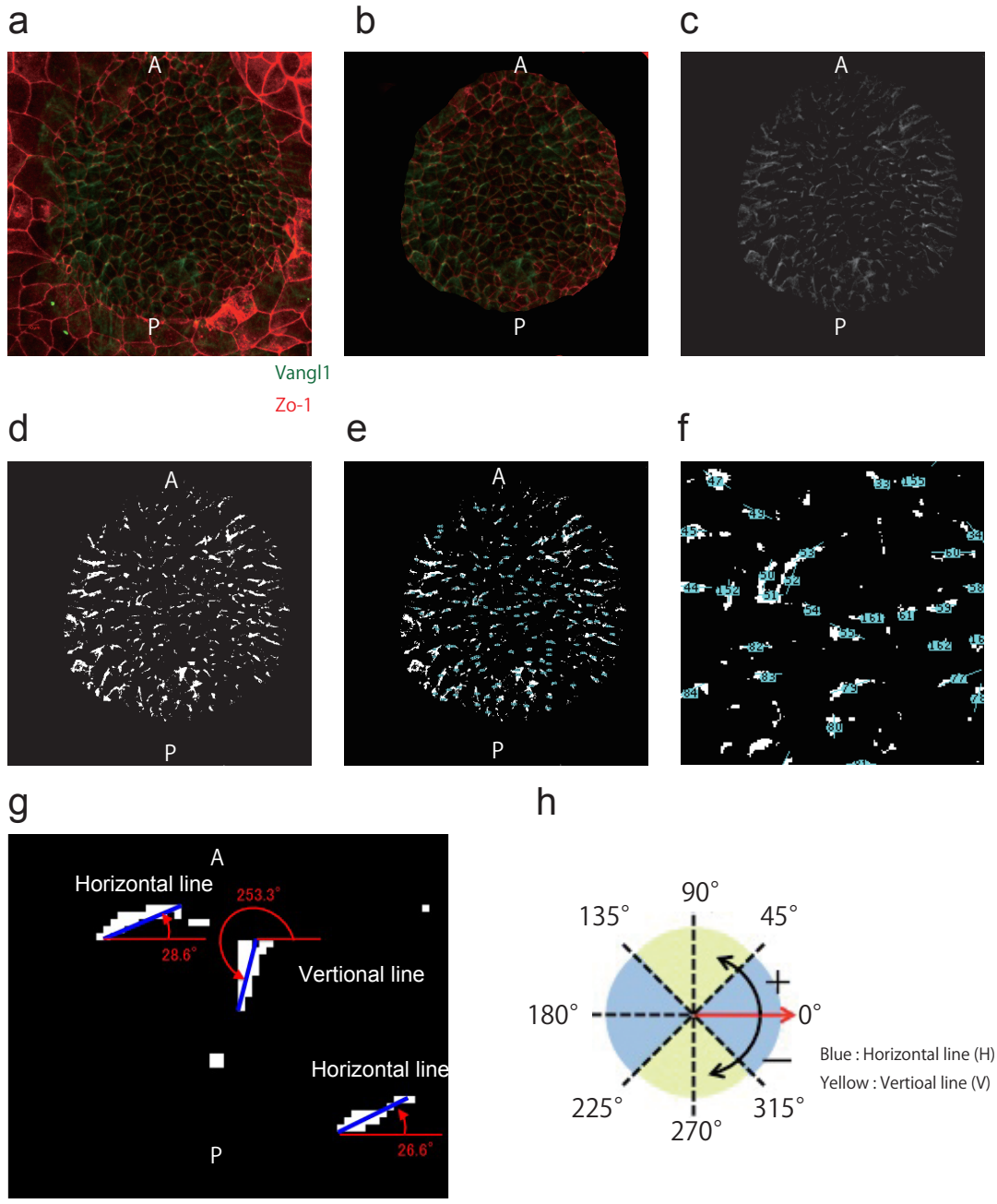

Figure S3 Quantification of PCP core protein distribution in the node using ImageJ

(a) Confocal image of the node immunostained for the Vangl1 (green) and Zo-1(red) at 3-5 So stage. **(b)** Only node excised from the confocal image, "node-image". **(c)** Image of only Vangl staining signal, "Vangl1-image". **(d)** Binarization using ImageJ software ,"binarization-image". **(e)** Tracing of the white lines with "Straight line selections" tool. **(f)** Enlarged view of (e). **(g)** Acquisition of the angles of each line using ImageJ software. **(h)** Angle between 0 ° ~ 45 ° , 135 ° ~ 225 ° and 315 ° ~360 ° are considered as horizontal. Angle between 45 ° ~ 135 ° and 225 ° ~ 315 ° are considered as vertical. The proportion between those two populations is estimated as a H/V rate.

ACKNOWLEDGEMENTS

I am deeply grateful to Pr. Hiroshi Hamada whose suggestions and support were inestimable value for my study.

My greatest appreciation goes to H. Shiratori, M. Hashimoto and R. Ajima whose comments made enormous contribution to my work. I am deeply grateful to S.Yoshiba and A. Kawasumi, who provided me with valuable comments, the psychological support and taught me the fundamental techniques. I am also indebted to all laboratory members for their comments and supports.

I want to thank L. Lamri and M. Boubakri who contributed in the correction of my dissertation. Without their help, this dissertation would not be materialized.

I am also indebted to Y. Yamamoto-Shiraishi (Nagoya University) and M.Komada (Aichi Gakuin University). They gave me supportive push in my initial steps five years ago.

Finally, I would also like to express my gratitude to my family for their financial support and warm encouragement.

This study was supported by CREST of the Japan Science and by GCOE of Osaka University.

REFERENCES

Agalliu, D., Takada, S., Agalliu, I., McMahon, A.P., and Jessell, T.M. (2009). Motor neurons with axial muscle projections specified by Wnt4/5 signaling. Neuron *61*, 708-720.

Antic, D., Stubbs, J.L., Suyama, K., Kintner, C., Scott, M.P., and Axelrod, J.D. (2010). Planar cell polarity enables posterior localization of nodal cilia and left-right axis determination during mouse and Xenopus embryogenesis. PloS one *5*, e8999.

Bastock, R., Strutt, H., and Strutt, D. (2003). Strabismus is asymmetrically localised and binds to Prickle and Dishevelled during Drosophila planar polarity patterning. Development *130*, 3007-3014.

Cartwright, J.H., Piro, O., and Tuval, I. (2004). Fluid-dynamical basis of the embryonic development of left-right asymmetry in vertebrates. Proceedings of the National Academy of Sciences of the United States of America *101*, 7234-7239.

Cha, J., Bartos, A., Park, C., Sun, X., Li, Y., Cha, S.W., Ajima, R., Ho, H.Y., Yamaguchi, T.P., and Dey, S.K. (2014). Appropriate crypt formation in the uterus for embryo homing and implantation requires Wnt5a-ROR signaling. Cell reports *8*, 382-392.

Cruciat, C.M., and Niehrs, C. (2013). Secreted and transmembrane wnt inhibitors and activators. Cold Spring Harbor perspectives in biology *5*, a015081.

Gao, B., Song, H., Bishop, K., Elliot, G., Garrett, L., English, M.A., Andre, P., Robinson, J., Sood, R., Minami, Y., *et al.* (2011). Wnt signaling gradients establish planar cell polarity by inducing Vangl2 phosphorylation through Ror2. Developmental cell *20*, 163-176.

Hashimoto, M., Shinohara, K., Wang, J., Ikeuchi, S., Yoshiba, S., Meno, C., Nonaka, S., Takada, S., Hatta, K., Wynshaw-Boris, A., *et al.* (2010). Planar polarization of node cells determines the rotational axis of node cilia. Nature cell biology *12*, 170-176.

Hayashi, S., Lewis, P., Pevny, L., and McMahon, A.P. (2002). Efficient gene modulation in mouse epiblast using a Sox2Cre transgenic mouse strain. Mechanisms of development *119 Suppl 1*, S97-S101.

Heisenberg, C.P., Tada, M., Rauch, G.J., Saude, L., Concha, M.L., Geisler, R., Stemple, D.L., Smith, J.C., and Wilson, S.W. (2000). Silberblick/Wnt11 mediates convergent extension movements during zebrafish gastrulation. Nature *405*, 76-81.

Majumdar, A., Vainio, S., Kispert, A., McMahon, J., and McMahon, A.P. (2003). Wnt11 and Ret/Gdnf pathways cooperate in regulating ureteric branching during metanephric kidney development. Development *130*, 3175-3185.

Mao, Y., Mulvaney, J., Zakaria, S., Yu, T., Morgan, K.M., Allen, S., Basson, M.A., Francis-West, P., and Irvine, K.D. (2011). Characterization of a Dchs1 mutant mouse reveals requirements for Dchs1-Fat4 signaling during mammalian development. Development *138*, 947-957.

Matakatsu, H., and Blair, S.S. (2004). Interactions between Fat and Dachsous and the regulation of planar cell polarity in the Drosophila wing. Development *131*, 3785-3794.

Matsuyama, M., Aizawa, S., and Shimono, A. (2009). Sfrp controls apicobasal polarity and oriented cell division in developing gut epithelium. PLoS genetics *5*, e1000427.

Nonaka, S., Tanaka, Y., Okada, Y., Takeda, S., Harada, A., Kanai, Y., Kido, M., and Hirokawa, N. (1998). Randomization of left-right asymmetry due to loss of nodal cilia generating leftward flow of extraembryonic fluid in mice lacking KIF3B motor protein. Cell *95*, 829-837.

Nonaka, S., Yoshiba, S., Watanabe, D., Ikeuchi, S., Goto, T., Marshall, W.F., and Hamada, H. (2005). De novo formation of left-right asymmetry by posterior tilt of nodal cilia. PLoS biology *3*, e268.

Qian, D., Jones, C., Rzadzinska, A., Mark, S., Zhang, X., Steel, K.P., Dai, X., and Chen, P. (2007). Wnt5a functions in planar cell polarity regulation in mice. Developmental biology *306*, 121-133.

Saburi, S., Hester, I., Fischer, E., Pontoglio, M., Eremina, V., Gessler, M., Quaggin, S.E., Harrison, R., Mount, R., and McNeill, H. (2008). Loss of Fat4 disrupts PCP signaling and oriented cell division and leads to cystic kidney disease. Nature genetics *40*, 1010-1015.

Saijoh, Y., Adachi, H., Mochida, K., Ohishi, S., Hirao, A., and Hamada, H. (1999). Distinct transcriptional regulatory mechanisms underlie left-right asymmetric expression of lefty-1 and lefty-2. Genes & development *13*, 259-269.

Satoh, W., Gotoh, T., Tsunematsu, Y., Aizawa, S., and Shimono, A. (2006). Sfrp1 and Sfrp2 regulate anteroposterior axis elongation and somite segmentation during mouse embryogenesis. Development *133*, 989-999.

Satoh, W., Matsuyama, M., Takemura, H., Aizawa, S., and Shimono, A. (2008). Sfrp1, Sfrp2, and Sfrp5 regulate the Wnt/beta-catenin and the planar cell polarity pathways during early trunk formation in mouse. Genesis *46*, 92-103.

Shiratori, H., and Hamada, H. (2006). The left-right axis in the mouse: from origin to morphology. Development *133*, 2095-2104.

Song, H., Hu, J., Chen, W., Elliott, G., Andre, P., Gao, B., and Yang, Y. (2010). Planar cell polarity breaks bilateral symmetry by controlling ciliary positioning. Nature *466*, 378-382.

Tao, H., Suzuki, M., Kiyonari, H., Abe, T., Sasaoka, T., and Ueno, N. (2009). Mouse prickle1, the homolog of a PCP gene, is essential for epiblast apical-basal polarity. Proceedings of the National Academy of Sciences of the United States of America *106*, 14426-14431.

Villano, J.L., and Katz, F.N. (1995). four-jointed is required for intermediate growth in the

proximal-distal axis in Drosophila. Development *121*, 2767-2777.

Yamaguchi, T.P., Bradley, A., McMahon, A.P., and Jones, S. (1999). A Wnt5a pathway underlies outgrowth of multiple structures in the vertebrate embryo. Development *126*, 1211-1223.

ACCOMPLISHMENT LIST

投稿論文等	発表論文誌の名称、巻、頁、発表年	共著者又は共同発表者氏名
Polarization of the mouse node cells by asymmetric distribution of Wnt5a/5b and their inhibitors	投稿準備中	Katsura Minegishi, Masakazu Hashimoto, Rieko Ajima, Katsuyoshi Takaoka, Kyosuke Shinohara, Yayoi Ikawa,1 Andrew McMahon, Akihiko Shimono, Hidetaka Shiratori, and Hiroshi Hamada
Self-regulated left-right asymmetric expression of Pitx2c in the developing mouse limb.	Developmental biology. 2014 Nov 15;395(2):331-41	Shiratori H, Yashiro K, Iwai N, Oki S, Minegishi K, Ikawa Y, Kanata K, Hamada H.
Prenatal findings in congenital leukemia: a case report.	Fetal diagnosis and therapy. 2011;29(4):325-30	Sato Y, Izumi Y, Minegishi K, Komada M, Yamada S, Kakui K, Tatsumi K, Mikami Y, Fujiwara H, Konishi I.

学会発表等	国際会議等の名称及び発表年月日	共著者又は共同発表者氏名
Extraction of DNA from human embryos after long-term preservation in formalin solution	第 115 回日本解剖学会総会・全国学術集会　ポスター発表 2010 年 3 月 28 日～30 日	峰岸かつら、　駒田致和、土屋真衣子、塩田浩平、山田重人
消化管原基の予定呼吸器領域を決定する因子の探索	第 31 回　日本分子生物学会年会 ポスター発表 2008 年 12 月 9 日～12 日	峰岸かつら、田中亜由美、山本茂樹、樋口裕明、平野みえ、黒岩厚